Rare Metal Materials and Engineering
Volume 52, Issue 6, June 2023
Available online at www.rmme.ac.cn

Science Press

Cite this article as: Li Boxin, Niu Jiale, Feng Zhibin, et al. Influence of Warm Rolling Path on Shear Strength of Explosively Welded Ti/Steel Clad Plate[J]. Rare Metal Materials and Engineering, 2023, 52(06): 2010-2016.

ARTICLE

Influence of Warm Rolling Path on Shear Strength of Explosively Welded Ti/Steel Clad Plate

Li Boxin[1], Niu Jiale[1], Feng Zhibin[1], Mo Taiqian[2], Wang Pengju[3]

[1] School of Materials Science and Engineering, Xi'an Polytechnic University, Xi'an 710048, China; [2] School of Mechanical Engineering, Guizhou University, Guiyang 550025, China; [3] Chongqing Hongjiang Machinery Co., Ltd, Chongqing 402160, China

Abstract: Explosively welded Ti/steel clad plates were one-pass warm rolled by 60%, microstructures of the Ti layer and steel layer adjacent to interface were investigated, and shear strength of the one-pass warm rolled clad plates was tested. Results show that the one-pass warm rolling process can cause obvious shear deformation in both the Ti layer and steel layer adjacent to the interface. Because of the shear deformation, the RD-split basal texture forms in the Ti layer. In the steel layer, high fraction of the rotated cube texture and low fraction of the γ fiber texture form. Compared with the common multi-pass rolling method, shear strength of the one-pass warm rolled Ti/steel clad plate is improved because the shear deformation refines the interfacial compounds.

Key words: one-pass warm rolling; shear deformation; microstructure; shear strength

Explosively welded bi-metal or multi-metal clad plates are often subjected to rolling process to enlarge dimension and to improve mechanical properties[1]. During rolling, temperature and reduction are two important parameters, which seriously affect microstructures and mechanical properties of the clad plates[2–4].

Normally, warm rolling is considered as an effective processing method for large scale industrial production. In the meanwhile, the process also has cost advantage[5–6]. It is reported that warm rolling can increase the crystal defects of the invar alloy (Fe-36.6Ni-1.5Cr-1.3Mo-1.1V-0.22C) and then improve the mechanical properties of the alloy. The invar alloy warm rolled at 750 °C presents the maximum ultimate strength of 921 MPa, increased by 21% compared to the alloy without warm rolling[7]. The 0.10C-0.32Si-1.50Mn-0.015P-0.003S-0.04Nb-0.06V-0.015Ti steel was warm rolled. Research results showed that the main mechanism of microstructure evolution during warm rolling is dynamic recovery. In the meanwhile, warm rolling can also refine grains. As a result, the warm rolled steel has greatly enhanced strength (64–158 MPa) compared to the conventionally rolled steel, and the warm rolled steel has high elongation in spite of high strength[8]. The warm rolled 9Mn steel was investigated by researchers, and results showed that the warm rolled 9Mn steel contains austenite and deformed ferrite/martensite. In addition, the occurrence of dynamic recovery during warm rolling results in a low storage energy of recrystallization. Consequently, the warm rolled and annealed 9Mn steel shows a better combination of ultimate tensile strength (1380 MPa) and total elongation (29.11%)[9].

Large strain rolling is a high efficiency rolling process, which can refine grains and improve mechanical properties of metallic materials[10]. For example, AA7020 plates were warm rolled, and research results showed that the increase in rolling reduction causes long strip grains. An increase in the rolling reduction improves the mechanical properties of the AA7020 alloy[11]. The ZK60 alloy was warm rolled, and results showed that with the increase in rolling reduction, the hardness and tensile strength of the alloy increase, and the rolling process improves the workability of the ZK60 alloy[12].

Warm rolling can improve elongation and strength of metallic materials. At the same time, large strain rolling can also improve the mechanical properties of metallic materials. Normally, the warm rolling and large strain rolling are often used to process single metallic materials, and the effect of

Received date: October 25, 2022
Foundation item: Natural Science Basic Research Program of Shaanxi Province (2022JQ-466); Doctoral Scientific Research Foundation of Xi'an Polytechnic University (107020535)
Corresponding author: Li Boxin, Ph. D., School of Materials Science and Engineering, Xi'an Polytechnic University, Xi'an 710048, P. R. China, Tel: 0086-29-82330167, E-mail: boxin-li@xpu.edu.cn

warm rolling and large strain rolling on mechanical properties of bi-metal clad plates is still unclear. For the clad plates, interface is an important structure, the warm rolling and large strain rolling can affect the interface and then affect the mechanical properties of bi-metal clad plates. In the present study, explosively welded Ti/steel clad plates were warm rolled at 450 ° C. In order to investigate the influence of rolling path on shear strength of the plate, two different rolling paths, i. e. one-pass rolling and nine-passes rolling were applied. The interface and the microstructure adjacent to the interface of the warm rolled clad plates were studied, and the shear strength of the warm rolled clad plates was tested.

1 Experiment

The explosively welded Ti/steel plates (50 mm×10 mm×5.6 mm, thickness of the Ti layer was 2.8 mm) were chosen as the raw materials. The chemical compositions (wt%) of the Ti were 0.06 Fe, 0.01C, 0.01 N, 0.01 H, 0.08 O and the balance Ti. The steel was composed of 0.15 C, 0.23 Si, 0.67 Mn and the balance Fe (wt%).

The plates were heated to 450 °C in an argon filled furnace before rolling. Fig. 1 shows the technological process of the one-pass rolling or nine-passes rolling. In order to facilitate the rolling, the front of the samples was cut into wedge shape. The Ti/steel clad plate was rolled to 2.8 mm by one pass (the rolled plate was labeled as 1P-60) or nine passes (the rolling reduction for each pass was 10%, the last pass was 7%, and the rolled plate was labeled as 9P-60), and the rolling reduction was 60%.

Microstructure of the warm rolled clad plates was studied by scanning electron microscope (SEM, JEOL JSM-7900F). Samples for the SEM observation were ground by abrasive papers and then polished by a diamond polishing spray (0.25 μm). The chemical element distribution of the samples was detected by energy-dispersive spectroscopy (EDS). Electron backscattered diffraction (EBSD, Oxford Instruments, Nordlys Max^3) was also used to reveal the microstructure of the samples adjacent to the interface. Samples for EBSD characterization were ground and electro-polished. The electrolyte for the polishing was a mixture of methanol (60 mL), butoxyethanol (34 mL), and perchloric acid (6 mL). Electro-polishing was conducted at 18 V with an electric current of 0.4 A and a polishing time of 30 s. The EBSD data were obtained by an indexing step of 1.0 μm and analyzed using HKL® Channel 5 software.

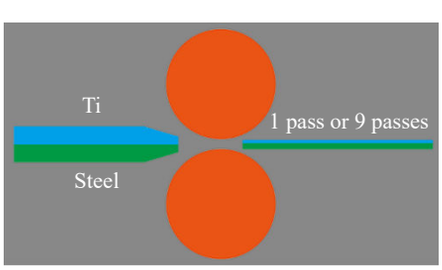

Fig.1 Diagram of one-pass rolling or nine-passes rolling

The shear strength of the warm rolled clad plates was tested by tensile shear test. Sample for the tensile shear test is shown in Fig.2. Each sample was tested by three times, and the final shear strength of the sample was the mean value. A Vicker's hardness tester was used to test the hardness of the samples. The load was 100 g, the holding time was 10 s, and the distance between the test points was 25 μm.

Strain distribution conditions of samples during one-pass polling and the first pass of the nine-passes rolling were obtained by finite element (Deform-3D) method. The inseparable Ti and steel were defined as the deformation parts. However, the rollers were defined as rigid. The friction contact between the Ti layer and steel layer and the rollers was defined to ensure authenticity of the simulation.

2 Results

2.1 Microstructure of Ti adjacent to interface

Fig.3 shows the inverse pole figure (IPF) of Ti adjacent to the Ti/steel interface in different samples. Grains in both the 1P-60 and 9P-60 samples are seriously deformed, and high density of low angle grain boundaries (LAGBs) are observed in the deformed grains. In the 1P-60 sample, as shown in Fig.3a, obvious shear bands (circled by white dotted line) are observed, which indicate that shear deformation is activated. Grain size of the 1P-60 sample is not uniform, grains of the shear bands are smaller than grains not in the shear bands. However, in the 9P-60 sample, as shown in Fig.3b, grain size is homogeneous, and obvious shear deformation is not observed.

The {0001} pole figures of Ti adjacent to the Ti/steel interface in different samples are shown in Fig.4. In both the samples, a normal texture of Ti after rolling, namely the TD-split basal texture, is identified. The basal poles of Ti tilt away from the normal direction (ND) to the transverse direction (TD). In the meanwhile, the basal poles of Ti also tilt from the ND to the rolling direction (RD) to form the RD-split basal texture. The tilted angle of the RD-split basal texture in the two samples is different, which is 29° in the 1P-60 sample and 24° in the 9P-60 sample.

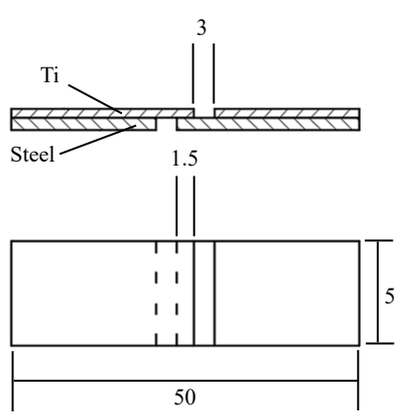

Fig.2 Sample for the tensile shear test

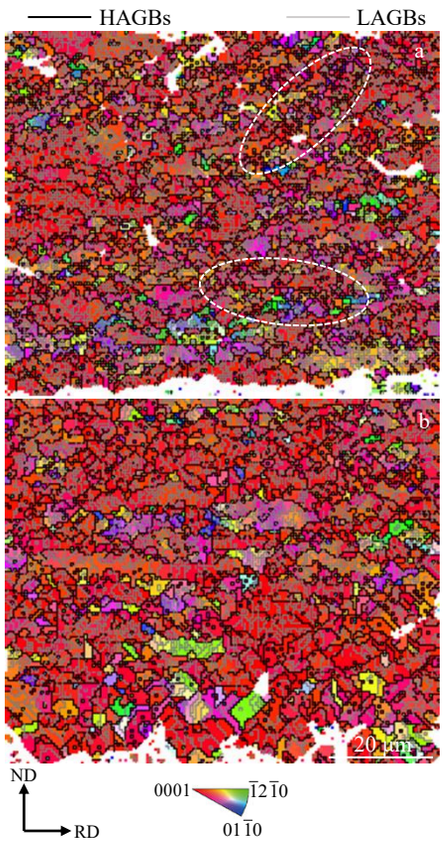

Fig.3 IPF of Ti adjacent to the Ti/steel interface: (a) 1P-60 sample and (b) 9P-60 sample

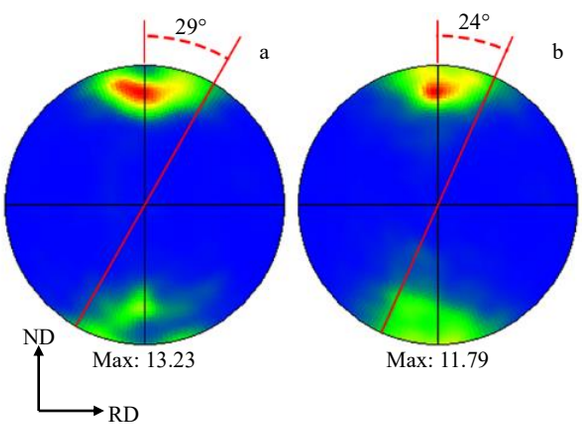

Fig.4 {0001} pole figures of Ti adjacent to the Ti/steel interface: (a) 1P-60 sample and (b) 9P-60 sample

2.2 Microstructure of steel adjacent to interface

Fig. 5 shows the IPFs of steel adjacent to the Ti/steel interface in different samples. In the 1P-60 sample, as shown in Fig.5a, shear deformation is also identified, and shear bands containing fine grains are observed. In the 9P-60 sample, as shown in Fig.5b, grains are elongated along the RD, and shear bands are not observed.

Fig. 6 shows the φ_2=45° sections in ODFs of steel adjacent to the Ti/steel interface in different samples. Three main textures, i. e. rotated cube texture ({001}<110>), and γ-fiber texture ({111}<112> and {111}<110>) are identified in both the samples, and the texture kind is same. However, the fraction of different textures in the two samples is different. Fig. 7 shows the texture fraction in different samples. In the 1P-60 sample, the fraction of the rotated cube texture is higher than that in the 9P-60 sample. On the contrary, the fraction of the γ-fiber texture in the 1P-60 sample is lower than in the 9P-60 sample.

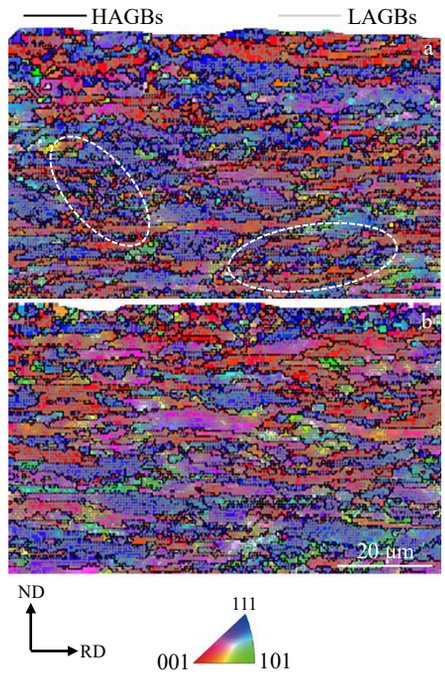

Fig.5 IPFs of steel adjacent to the Ti/steel interface: (a) 1P-60 sample and (b) 9P-60 sample

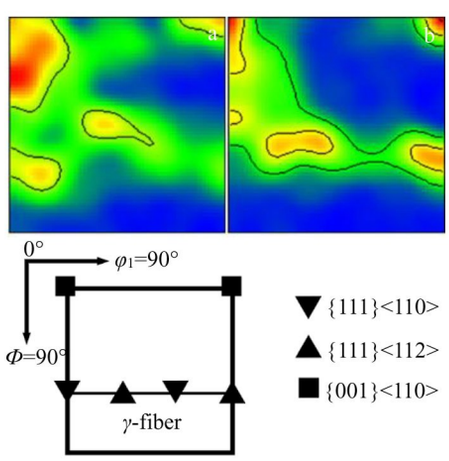

Fig.6 φ_2=45° sections in ODFs of steel adjacent to the Ti/steel interface: (a) 1P-60 sample and (b) 9P-60 sample

2.3 Microstructure of interface

Backscattered electron images of the Ti/steel interface in different samples are shown in Fig. 8. In both the samples, the

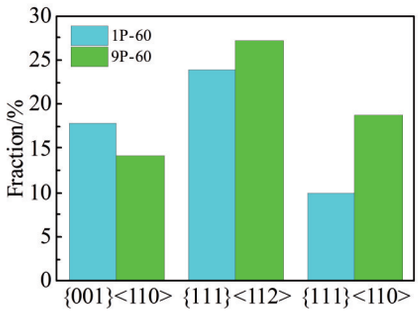

Fig.7 Texture fraction of different samples

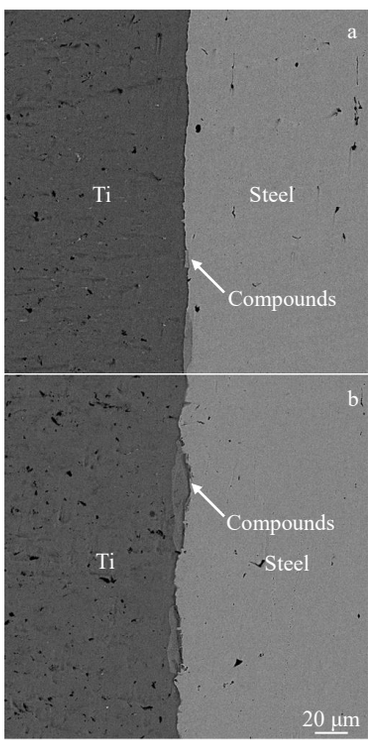

Fig.8 Backscattered electron images of the Ti/steel interface: (a) 1P-60 sample and (b) 9P-60 sample

Ti/steel interfaces are intact, and flaws such as cracks, voids are not observed. Interfacial compounds are observed at the interface. In the 1P-60 sample, the size of the compounds is small. However, in the 9P-60 sample, the size of the interfacial compounds is much larger.

2.4 Mechanical properties

Shear strengths of different samples are shown in Fig.9. The mean shear strength of the 1P-60 sample is 266.8 MPa. Mean shear strength of the 9P-60 sample is lower, 188.7 MPa.

Fig. 10 shows the hardness of different samples adjacent to the interface. Apparently, in both the Ti layer and the steel layer, hardness value of the 1P-60 sample is higher than that of the 9P-60 sample.

3 Discussion

Fig. 11 shows the equivalent strain distribution of Ti in the two samples during rolling. In the 1P-60 sample, as shown

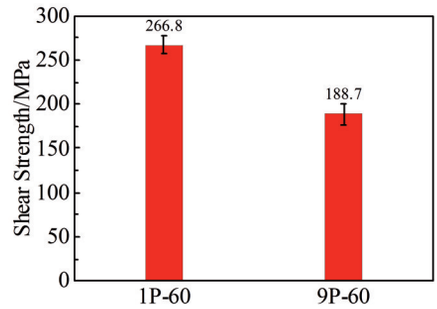

Fig.9 Shear strength of different samples

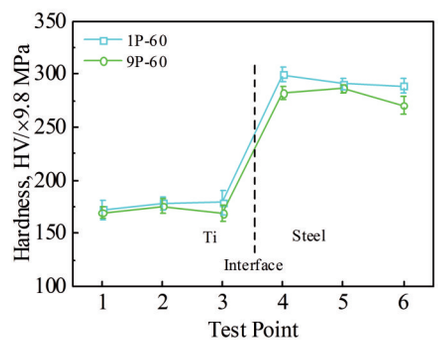

Fig.10 Hardness of different samples adjacent to the interface

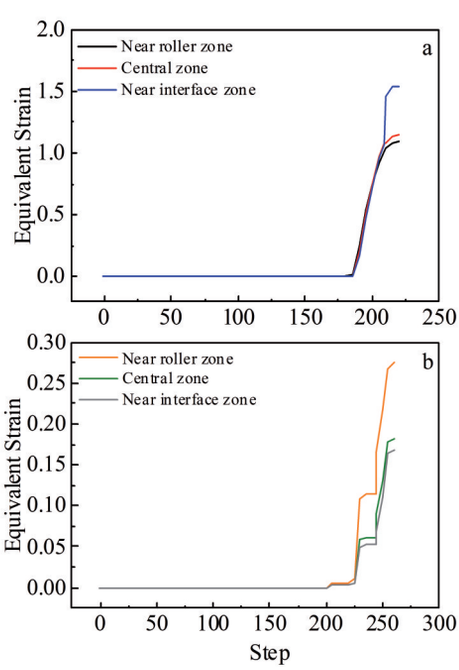

Fig.11 Equivalent strain distribution of Ti in different zones of 1P-60 sample (a) and 9P-60 sample (b) during rolling

in Fig. 11a, the near interface zone shows an enlargement in strain compared with the near roller zone and the central zone. On the contrary, in the 9P-60 sample, as shown in Fig.11b, the near roller zone shows a surge in strain compared with the central zone and the near interface zone. In Fig. 12, the strain distribution of the steel layer is similar to that of the

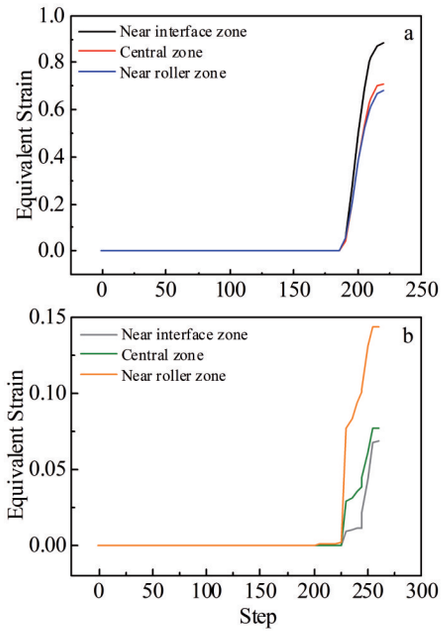

Fig.12 Equivalent strain distribution of steel in different zones of 1P-60 sample (a) and 9P-60 sample (b) during rolling

Ti layer.

In the 1P-60 sample, the increase in strain of the near interface zone results in shear deformation in the Ti layer and the steel layer, as shown in Fig. 3a and Fig. 5a. It has been reported that shear deformation can refine grains[13–14], so fine grains are observed in the shear bands. In the 9P-60 sample, because the rolling reduction is small, obvious deformation only happens in the near roller zone. As a result, no obvious shear deformation is observed in Fig.3b and Fig.5b.

The shear deformation also affects the grain orientation of the Ti layer and steel layer. During shear deformation, the basal slip planes of Ti are tilted from ND to RD. As a result, the RD-split basal texture forms[15]. As the 1P-60 samples go through obvious shear deformation, the tilted angle in Fig. 4a is bigger than that in Fig. 4b. In the steel layer, it is reported that the rotated cube texture ({001}<110>) is sensitive to the shear deformation, the texture is often identified at the location underwent shear deformation[16]. Because the near interface zone in the 1P-60 sample possesses obvious shear deformation, the texture fraction in this sample is larger as shown in Fig. 7. Earlier research results also showed that the shear deformation can promote the translation of the γ fiber texture to other textures[17]. As a result, in Fig.7, the fraction of the γ fiber texture in the 1P-60 sample is lower than that in the 9P-60 sample.

The normal interfacial compounds at the Ti/steel interface include TiC, FeTi, and Fe_2Ti, which possess extremely high hardness value and poor deformation ability[18–20]. During rolling, in the 1P-60 sample, because the most obvious shear deformation occurs at the near interface zone in the Ti layer and steel layer, stress concentration occurs at the interface. As a result, in Fig. 8a, the compounds break into smaller pieces. On the contrary, deformation of the near interface zone in the Ti layer and steel layer in the 9P-60 sample is inconspicuous, and the strain and stress concentration at the interface are small. As a result, in Fig. 8b, the large size compounds are remained[21].

Fig. 13 shows the morphologies and element distribution map of fracture after tensile shear test for different samples. In Fig.13a and 13b, both the Ti layer and the steel layer show the presence of Ti element, while the Fe element is not detected, which means that the fracture occurs at the Ti layer adjacent to the interface. As shown in Fig. 13c and 13d, in the 9P-60 sample, both the fracture surfaces show the presence of Ti and Fe elements, indicating that fracture occurs at the Ti/steel

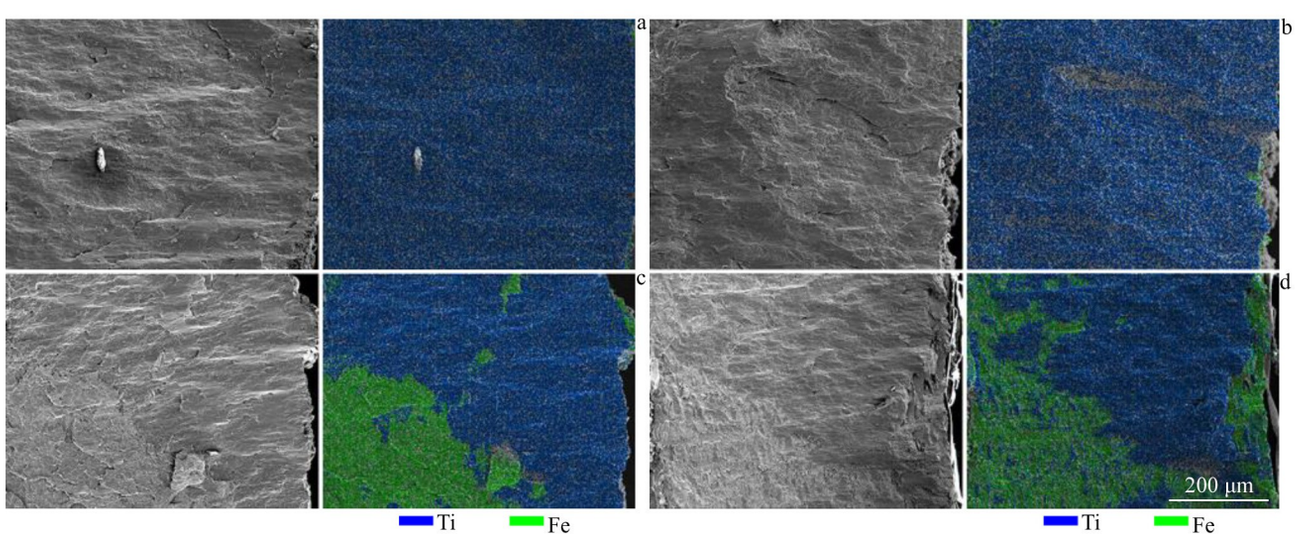

Fig.13 Morphologies and element distribution maps of fracture after tensile shear test of 1P-60 sample (a–b) and 9P-60 sample (c–d): (a, c) Ti layer and (b, d) steel layer

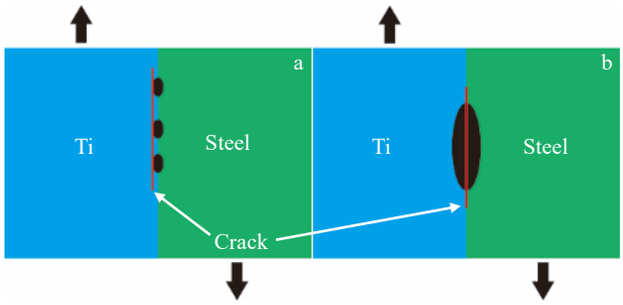

Fig.14 Crack propagation path in 1P-60 sample (a) and 9P-60 sample (b) during tensile shear test

interface. The crack propagation path during tensile shear test is shown in Fig.14. In the 1P-60 sample, because the size of interfacial compounds is smaller, they can strengthen the interface[22]. As a result, the fracture turns to translate along the Ti layer which possesses lower strength compared to the steel layer[23]. However, in the 9P-60 sample, the size of the interfacial compounds is larger, so they cannot withstand deformation, and thus micro-cracks occur in the compounds and converge at the interface. The spread of the crack at different zones leads to different shear strengths of the two samples. The Ti layer in the 1P-60 sample possesses higher strength compared to the interface of the 9P-60 sample, so the 1P-60 sample possesses higher shear strength value.

4 Conclusions

1) Explosively welded Ti/steel clad plate can be warm rolled by 60% in one rolling pass.

2) The one-pass warm rolling process can cause obvious shear deformation in both the Ti layer and steel layer adjacent to the interface. As a result, in the Ti layer, the RD-split basal texture forms. In the steel layer, high fraction of the rotated cube texture ({001}<110>) and low fraction of the γ fiber texture ({111} <112> and {111} <110>) are observed.

3) The interfacial compounds are refined by the shear deformation in the one-pass warm rolled Ti/steel clad plate. The interface strengthened by fine interfacial compounds can withstand larger loads without cracking. Shear strength of the one-pass warm rolled Ti/steel clad plate is improved.

References

1 Yang X, Shi C G, Fang Z H *et al. Materials Research Express*[J], 2019, 6: 26 519

2 Huang Q X, Zhang J, Zhu L *et al. Rare Metal Materials and Engineering*[J], 2017(7), 46(7): 1749

3 Chen Z Q, Liang W, Yu B *et al. Rare Metal Materials and Engineering*[J], 2015, 44(3): 587

4 Pang X X, Liu T T, Yin C G *et al. Rare Metal Materials and Engineering*[J], 2011, 40(10): 1718

5 Du J L, Li J, Feng Y L *et al. Materials and Design*[J], 2022, 221: 110 953

6 Storojeva L, Ponge D, Kaspar R *et al. Acta Materialia*[J], 2004, 52: 2209

7 Yao Y F, Zhao Q, Zhang C D *et al. Journal of Materials Research and Technology*[J], 2022, 19: 3046

8 Shen X J, Tang S, Wu Y J *et al. Materials Science and Engineering A*[J], 2017, 685: 194

9 Yan N, Di H S, Misra R D K *et al. Materials Science and Engineering A*[J], 2020, 796: 140 051

10 Wang K, Wang J F, Peng X *et al. Materials Science and Engineering A*[J], 2019, 748: 100

11 Xu Z, Zhu L H, Wang H B *et al. Journal of Materials Engineering and Performance*[J], 2021, 30: 8579

12 Gong X B, Gong W T, Kang S B *et al. Materials Research*[J], 2015, 18(2): 360

13 Sun J L, Trimby P W, Yan F K *et al. Acta Materialia*[J], 2014, 79: 47

14 Chen H M, Yu H S, Kang S B *et al. Rare Metal Materials and Engineering*[J], 2011, 40: 1708

15 Wang X X, Zhan M, Fu M W *et al. Journal of Materials Processing Technology*[J], 2018, 261: 86

16 Kang C G, Kang H G, Kim H C *et al. Journal of Materials Processing Technology*[J], 2007, 187–188: 542

17 Dorothee D, Stefan Z, Dierk R. *Acta Materialia*[J], 2007, 55: 2519

18 Marcin W, Michal G, Tomasz S *et al. Journal of Materials Engineering and Performance*[J], 2017, 26: 945

19 Aslan M, Michael S, Nachum F. *Acta Materialia*[J], 2014, 75: 348

20 Prasanthi T N, Sudha C, Saroja S. *Metallurgical and Materials Transactions A*[J], 2017, 48: 1969

21 Ji C, Huang H G, Sun, J N *et al. Journal of Manufacturing Processes*[J], 2018, 34: 593

22 Vamsi Krishna B, Praveen K, Venugopal P *et al. Materials Science and Engineering A*[J], 2005, 394: 277

23 Chang H, Zheng M Y. *Rare Metal Materials and Engineering*[J], 2016, 45(9): 2242

温轧路径对钛/钢爆炸复合板抗剪切强度的影响

李博新[1]，牛嘉乐[1]，封志斌[1]，莫太骞[2]，王鹏举[3]
(1. 西安工程大学 材料工程学院，陕西 西安 710048)
(2. 贵州大学 机械工程学院，贵州 贵阳 550025)
(3. 重庆宏江机械有限公司，重庆 402160)

摘　要：对爆炸复合的钛/钢复合板进行了一道次60%的温轧，研究了一道次温轧钛/钢爆炸复合板的近界面微观组织及剪切强度。结果显示，一道次温轧工艺可以引起钛层和钢层近界面组织的显著剪切变形。由于剪切变形，钛层形成了RD分散织构。钢层含有高组份的旋转立方织构及低组份的γ纤维织构。对比常规多道次轧制方法，由于剪切变形可细化界面化合物，使得一道次温轧钛/钢复合板抗剪切强度得到提升。

关键词：一道次温轧；剪切变形；微观组织；抗剪切强度

作者简介：李博新，男，1990年生，博士，西安工程大学材料工程学院，陕西 西安 710048，电话：029-82330167，E-mail：boxin-li@xpu.edu.cn